PREDICTIVE CAPABILITY OF NONLINEAR STATIC ANALYSIS PROCEDURES FOR SEISMIC EVALUATION OF BUILDINGS

Dionisio Bernal[1] and Arash Nasseri[2]

[1] Civil and Environmental Engineering Department, Center for Digital Signal Processing, Northeastern University, Boston, MA.
[2] Graduate Student, Northeastern University, Boston, MA,

Abstract

The recorded response of a number of reinforced concrete buildings to real earthquakes are used to test the predictive capability of nonlinear static procedures (NSP). Response parameters such as drifts and inter-story shears are obtained by blending measured acceleration signals and model based information, using an observer. The buildings are represented by 3D nonlinear Finite Element models with elastic stiffness updated from eigenproperties identified from small amplitude response. The fidelity of the models for behavior at large amplitudes is validated by contrasting time history predictions with measured strong motion acceleration response. As one anticipates from theoretical considerations, the prediction accuracy of NSP is found to be significantly higher in the lower levels of the buildings considered. The ratio of "measurements" to predictions over the full height for the cases analyzed has a mean and coefficient of variation of around {1.05 and 0.22} for shears and {1.2 and 0.45} for inter-story drifts. Differences in predictive capability between the various NSP are found statistically insignificant.

Introduction

Many existing concrete buildings in the US were designed and built without the benefit of the modern understanding of behavior for severe seismic loading. Since an across the board policy of condemnation or mandatory retrofit of the old stock is economically unacceptable, a case by case determination of vulnerability has proven necessary. The framework that has evolved is one where building performance is explicitly quantified in terms of anticipated damage and decisions are made on this basis. Ideally the anticipated performance would be evaluated by subjecting a refined nonlinear model of the structure to an ensemble of multi-component excitations representing the appropriate level of shaking. At present, however, the nonlinear dynamic approach is considered impractical for routine applications. The procedures that have emerged as a compromise between a code-based evaluation and time history analysis of nonlinear Finite Element models have been labeled Nonlinear Static Procedures (NSP).

In NSP the connection between structural behavior and response amplitude is modeled explicitly but, as the name indicates, the dynamics are avoided by assuming that the results of interest can be taken from configurations reached when the structure is pushed laterally using one or more prescribed lateral load distributions. Recently the Applied Technology Council (ATC) undertook a study to examine the variability of predictions from different guidelines and suggested changes geared towards reducing the differences between the techniques currently in

vogue [1]. This paper summarizes some results obtained in a CSMIP funded project whose objective was to examine the relative merit of NSP in light of empirical data available from the response of structures to real earthquakes. This assessment has two distinct components, namely:

1. Obtaining the NSP predictions

2. Obtaining estimates of the quantities of interest from the acceleration data.

The uncertainties that appear in item#1 due to modeling difficulties are well appreciated but the issues connected with item#2 are less so. It is, in fact, not uncommon in the literature to find references to "measured base-shear" or to "measured inter-story drift" even though these quantities are not actually measured. In this regard the paper shows that the procedure used to make inferences from the acceleration data can have an important effect on accuracy. In this study the response is reconstructed from the measurements using an observer having a gain that accounts for the fact that the bulk of the discrepancies between measurements and open loop model estimates arise (in this application) from modeling errors [2]. The rest of the paper is organized as follows. The first section summarizes the conceptual support of NSP and the next outlines the observer. Results for the 13-story Sherman Oaks building, the 6-story Imperial County Services building and a 4-story telephone building in Watsonville are presented subsequently. Two other structures are presented in the final report of the project to CSMIP, namely, a 3-story building in Santa Barbara and a 20-story structure in North Hollywood [3]. The paper closes with a brief critical review of the material presented.

Nonlinear Static Procedures

Assume the performance of a structure during earthquakes is some function of a set of variables $r_1(t)$ $r_2(t)$ … $r_n(t)$ and that an approximate but practically useful decision on the structural state can made by looking at some metric from each variable separately, typically the maximum value. Say these metrics are r_1, r_2 .. r_n. The objective of NSP is to provide and estimate of r_j from a static analysis of the structure subjected to a prescribed lateral load distribution. In principle the lateral load distribution can be different for each r_j, but in practice only a few load patterns, and many times only one, are used. NSP differ on the criterion that is used for deciding the magnitude of the load at which the analysis is terminated. At present all techniques provide termination in terms of the attainment of a roof displacement that is referred to as the target displacement or the performance point. There are two NSP in vogue: the coefficient method CM and the capacity spectrum method CSM.

The Coefficient Method (FEMA-356 and FEMA-440 CM)

In this method the target displacement is determined using the formula

$$\delta_t = C_o C_1 C_2 C_3 S_a \frac{T_e^2}{4\pi^2} g \qquad (1)$$

where C_o= ratio between the MDOF roof displacement and the SDOF elastic spectral response, C_1 = ratio between the expected maximum displacement of the inelastic SDOF oscillator with

elastic perfectly plastic (EPP) hysteretic to the displacements calculated for linear elastic response, C_2 = factor that accounts for deviations of the hysteretic response from the ideal EPP behavior and C_3 = amplification factor for P-Δ effects. The factor C_3 has been suspect to be near one since the early work of Husid, and Jennings and Husid [4,5] and the extensive MDOF studies in the 1990's by Bernal provide further confirmation [6,7]. In the newest version of the coefficient method C_3 has be eliminated and replaced by a minimum strength requirement and the numerical values of the coefficients C_1 and C_2 have been adjusted [8]. The remaining variables in eq.1 are S_a = elastic response spectrum acceleration at the fundamental period T_e of the building, and g = acceleration of gravity.

Capacity-Spectrum Method (ATC-40 and FEMA-440 Linearization)

The basic assumption here is that the target displacement can be estimated from the maximum displacement of a linear elastic SDOF system having a damping and period that are larger than the values connected with the first mode of the elastic model of the building. The values of effective period and damping in the CSM need to be obtained iteratively because the "correct values" depend on the performance point and this is unknown at the outset. As noted in FEMA-440, many engineers prefer to work with the CSM because the graphical nature of the procedure is intuitively appealing. It is worth noting, however, that the impression of precision that comes from a solution that is obtained at the intersection of demand and capacity lines is not substantiated by examination of the theory. The new version of the CSM presented in FEMA-440 involves changes in the expression for the linearization parameters.

Applicability of NSP

Since NSP are founded on the assumption that the response can be "reasonably" approximated using a SDOF they become progressively less tenable as the influence of higher mode increases. FEMA 356 explicitly states that NSP shall be permitted for structures in which the effects of higher modes are not significant [9]. According to FEMA 356 the effects of higher modes are deemed significant if the story shear obtained from a response spectral analysis that captures at least 90% of the mass participation is ≥ than 1.3 times the same story shear obtained from a modal analysis based on the 1st mode. If the effect of higher modes is large, however, an NSP evaluation is still permitted by FEMA-356 but it must be accompanied by linear dynamic analysis. Acceptance criteria for the linear dynamic analysis are also provided. In the equivalent linearization procedures applicability is indirectly imposed by limiting the range of the expressions for the equivalent parameters to buildings with fundamental periods that do not exceed 2.0 seconds.

Estate Estimation in Earthquake Engineering

The sensors available on instrumented buildings do not provide a direct measurement of most of the quantities of interest and it is thus necessary to bring analytical tools to obtain estimations. Needless to say, if one had a perfect model and a very accurate description of the excitation all quantities could be taken from a simulated response. This, however, is far from the

situation that prevails in practice. The classical tool used for blending measurements with model information is known as an observer. A classical full order observer has the form

$$\hat{x}_{k+1} = A\,\hat{x}_k + Bu_k + G(y_k - \hat{y}_k) \tag{2}$$

where $\hat{x}$ is the state vector estimate, y is the measured output, $\hat{y}$ is the estimated output and the system is assumed to be described by the triple {A, B, C} where these matrices are, in the order given: the system matrix, the input to state matrix and the state to output matrix, respectively [10]. Eq.2 can also be written as

$$\hat{x}_{k+1} = (A - GC)\,\hat{x}_k + Bu_k + G y_k \tag{3}$$

where G is selected to attain specific goals. In particular, when uncertainties arise because of unknown initial conditions G is selected to bring the poles of the matrix in parenthesis in eq.3 close to the origin. When the bulk of the uncertainty arises because there are unmeasured disturbances (unmeasured inputs, for example) then, provided the disturbances are broad band the optimal gain is the Kalman Filter. In the application of interest here, however, much of the uncertainty comes from model errors and as a consequence the Kalman Filter (at least in standard form) is not applicable. An observer explicitly designed for the situation of large modeling error was recently proposed in [2] and has the form

$$\hat{x}_{k+1} = (I - C^T C)A\hat{x}_k + (I - C^T C)Bu_k + C^T y_{k+1} \tag{4}$$

where

$$A = \begin{bmatrix} 0 & I \\ -M^{-1}K & -M^{-1}C_D \end{bmatrix} \quad B = \begin{bmatrix} 0 \\ -r \end{bmatrix} \quad C = \begin{bmatrix} 0 & L \end{bmatrix} \tag{5a,b,c}$$

In the previous expressions M, C_D and K are the mass damping and stiffness matrices, u_k is the vector of ground accelerations, r is the pseudo-static displacement influence matrix and L is a Boolean matrix indicating which degrees of freedom (DOF) are measured. For example, if the 5th and the 9th DOF are measured then the (1,5) and (2,9) entries of L are unity and all others are zero. The form in eq.5 indicates that the state is the collection of relative displacements and relative velocities and eq.5c (in particular) shows that the measurements are assumed to be relative velocities. Needless to say, in practice the actual measurements are absolute accelerations but velocities in the bandwidth of interest can be computed with good accuracy from the accelerations and the form of the observer with velocity measurements is simpler. The feedback nature of an observer structure is illustrated schematically in Fig.1.

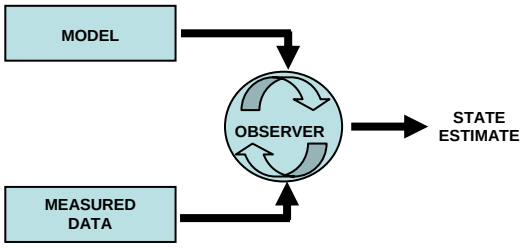

Fig.1 Schematic illustration of an observer.

Modal Projection Estimation

A solution to the estimation problem that is simpler than the observer is a projection of the measurements in a modal basis. We comment on this solution because it is often presented in the literature as accurate, yet, as we shall illustrate next, this may or may not be the case. The projection idea is simple, namely, with the response y(t) expressed in modal coordinates Y(t) one has

$$y(t) = \Phi Y(t) \tag{6}$$

where Φ is the modal matrix. Writing eq.6 in partitioned form

$$\begin{Bmatrix} y_m(t) \\ y_u(t) \end{Bmatrix} = \begin{bmatrix} \phi_{mm} & \phi_{mu} \\ \phi_{um} & \phi_{uu} \end{bmatrix} \begin{Bmatrix} Y_m(t) \\ Y_u(t) \end{Bmatrix} \tag{7}$$

where the subscripts *m* and *u* refer to measured and unmeasured coordinates one concludes that the responses at the unmeasured coordinates are

$$y_u(t) = \phi_{um}\phi_{mm}^{-1}\, y_m(t) + (\phi_{uu} - \phi_{um}\phi_{mm}^{-1}\phi_{mu})Y_u(t) \tag{8}$$

The unmeasured coordinates in the modal projection scheme are estimated as the first term in eq.8, namely

$$\hat{y}_u(t) = \hat{\phi}_{um}\hat{\phi}_{mm}^{-1}\, y_m(t) \tag{9}$$

where the *hat* on the modal quantities is added to emphasize that these are not exact results but model estimates. The error in the modal projection estimation is thus given by

$$\varepsilon_u = \left(\phi_{um}\phi_{mm}^{-1} - \hat{\phi}_{um}\hat{\phi}_{mm}^{-1}\right) y_m(t) + (\phi_{uu} - \phi_{um}\phi_{mm}^{-1}\phi_{mu})Y_u(t) \tag{10}$$

which has two parts, the first coming from error in the shapes of the *m* modes used to project the response and the second from the truncated space. It is shown next that for some conditions the reconstruction error in the modal projection approach can be significant.

Example on Estimation

Consider a 6-story shear building where the nominal model has masses of unity and inter-story stiffness of 680 (in consistent units) but the actual inter-story stiffness and the masses are 680*[1.2, 0.90, 0.95, 1.1, 1, 0.85] and [0.95, 1.02, 0.96, 0.97, 1, 1.1]. We take the real structure as having 2% modal damping while the nominal model is assigned 5%. This last discrepancy is simplistic but it is intended to stress the fact that in practice one seldom has a good characterization of the damping. One can confirm that the real structure and the nominal model have a fundamental frequency of 1 Hz (a coincidence selected to simulate the fact that the model

is likely updated to match an identified fundamental period). We assume measurements are available at coordinates #1 and #2 and that there is interest in predicting the drift in the 5th floor. Fig.2 presents the comparison of the exact solution with the following estimations: a) modal projection, b) modal projection with the output pre-filtered to the bandwidth of the first two modes, c) observer and d) nominal model in open loop.

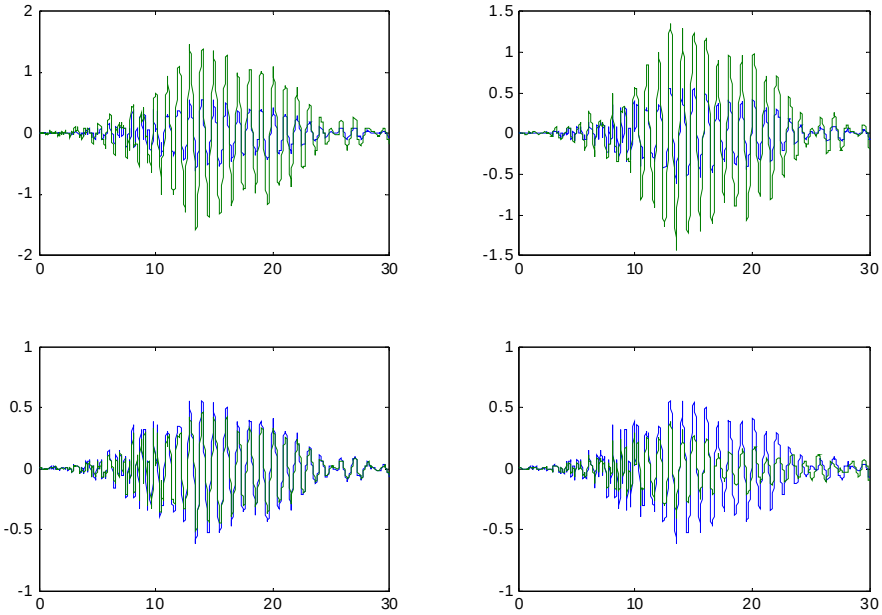

Fig.2 Drift on the 5th level: exact result in blue and predictions in green, sequentially from let to right by rows: a) MP, (b) FMP, (c) OB and (d) NM; drift in inches and time in seconds.

The superior accuracy of the observer prediction is evident by inspection.

Shearman Oaks

The Sherman Oaks building (CSMIP station number 24322) has13 stories above ground and two underground levels and was designed in 1964. The vertical load resisting system is concrete slabs (typically 4.5 inch thick) supported on concrete beams and columns and the lateral load resisting system is made up of moment resisting frames in both directions. The structure is on alluvium soil and the foundation is supported on concrete piles. The first floor spandrel girders were modified by post-tensioning after the 1971 San Fernando earthquake and in 1977 the building was instrumented with 15 sensors. Three sets of strong motion records are available, namely: Whittier (1987), Landers (1992) and Northridge (1994). No damage was reported due to the first two motions but the Northridge earthquake induced noticeable, yet repairable structural damage in the form of cracks in the beams, slabs, girders, and walls [11]. Fig. 3 depicts the instrumentation layout.

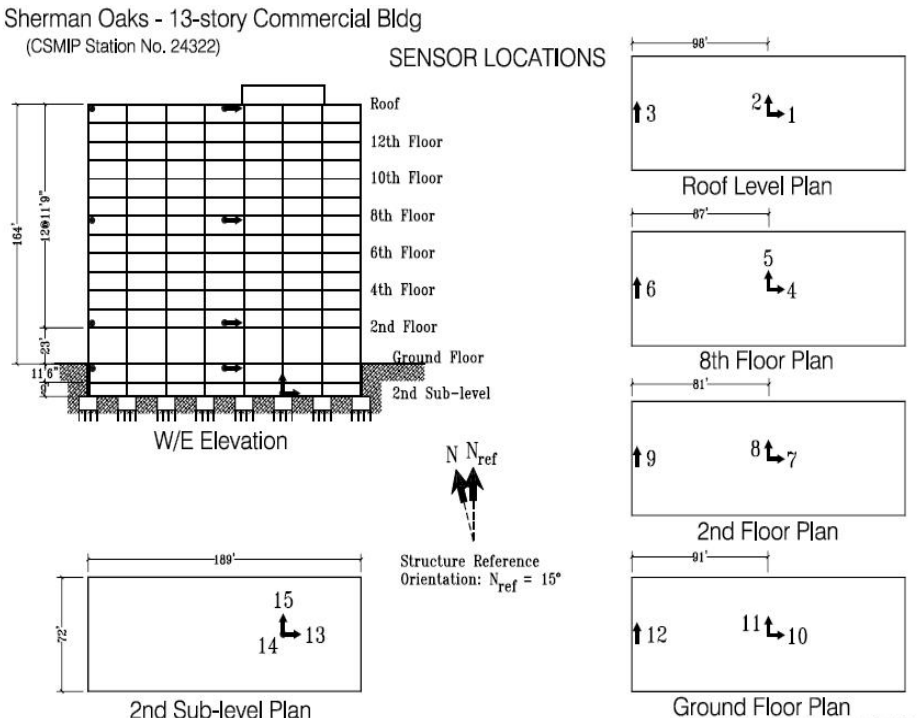

Fig.3 Layout of the sensors installed at Sherman Oaks building (taken from CSMIP web site).

Identification of modal properties and model updating

Identification of the quasi-linear properties of the building was done using the signals recorded during the Landers earthquake because this motion is closer in time to Northridge than Whittier and thus better captures the state of the system at the time of the shaking from Northridge. To increase confidence on the results the identification was carried out using various algorithms, in particular, ERA-OKID, Sub-ID and Reversed Time OKID [10,12]. It was found that the results for all the algorithms were quite close. The results shown in this section are those from the ERA-OKID algorithm [10].

Longitudinal Direction

The singular values of the Hankel matrix that is used to determine an effective model order showed 6 dominant directions, indicating 3 modes. Table1, taken directly from the ERA-OKID algorithm output summarizes the results obtained.

Table 1a. Poles in longitudinal direction

no.	Freq(Hz)	Damp%	cmi%	emac%	Mpcw%	mhp%	imp%	omp%	Msv%	mci%	moi%
1	0.386	5.363	95.6	95.6	100.0	100.0	100.0	100.0	100.0	19.5	0.2
2	1.382	6.338	9.5	9.5	99.8	76.3	76.8	99.3	52.3	41.0	0.2
3	2.520	6.839	0.0	0.0	97.8	0.0	0.0	83.1	41.6	59.5	0.1

Table 1b Mode shape amplitudes in the longitudinal direction, normalized to unity at the roof.

Level (see fig.2)	Channel #	Mode #1	Mode #2	Mode #3
2	Ch7	0.257	-0.854	0.917
8	Ch4	0.781	-0.515	-0.990
roof	Ch1	1	1	1

For a description of the quality indicators see [13].

Transverse Direction

Analysis showed that 3 modes could be reliably identified; results are summarized in Table 2.

Table 2a. Poles in transverse direction

no.	freq(Hz)	Damp%	cmi%	emac%	Mpcw%	mhp%	imp%	omp%	Msv%	mci%	moi%
1	0.358	4.974	90.9	90.9	100.0	99.9	99.9	100.0	100.0	15.3	0.2
2	2.357	5.814	7.6	7.7	98.9	40.4	45.8	88.3	47.6	45.9	0.2
3	1.321	6.936	43.1	43.8	98.3	85.1	85.7	99.3	53.8	35.7	0.1

Table 2b Mode shape amplitudes in the transverse direction, normalized to unity at the roof.

Level (see fig.3)	Channel #	Mode #1	Mode #2	Mode #3
2	Ch8	0.193	-0.645	1.010
8	Ch5	0.721	-0.669	-0.859
Roof	Ch2	1	1	1

Modeling of Basement Levels

A decision as to whether the model is to start at the ground floor or include the basement was made by looking at the Fourier amplitude spectrum of a pair of channels in each direction; one at the sublevel and one at the ground floor. The comparisons, which are shown in fig.4, illustrate that the spectra are essentially the same bellow 2.5 Hz. Since this bandwidth covers the first 3 modes in each direction a model that starts at the ground level is adequate.

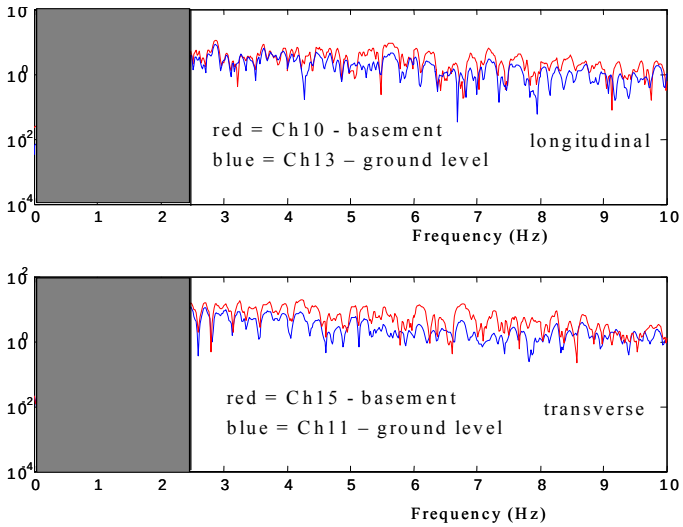

Fig.4 Fourier amplitude of channels at the lowest level (basement) and at the ground floor

Fictive Rotational Grounding

While the columns are taken to terminate at the ground level they cannot be treated as fixed since there is significant rotational flexibility at these points. Rotational support springs were thus included in the model. The initial stiffness of the springs was computed as the condensed flexural stiffness of a model of the basement frames. The spring constants, however, where subsequently treated as free parameters and adjusted to make the model fundamental frequency match the result from the system identification. The numerical values obtained are presented in the final report [3].

Development of Nonlinear Model

Nonlinear behavior was modeled with lump plasticity. The force-deformation relationship of plastic hinges was defined in terms of moment versus plastic rotation. The general force deformation relationships are as defined in FEMA 356 [9]. Strength degradation was modeled as shown schematically in fig.5.

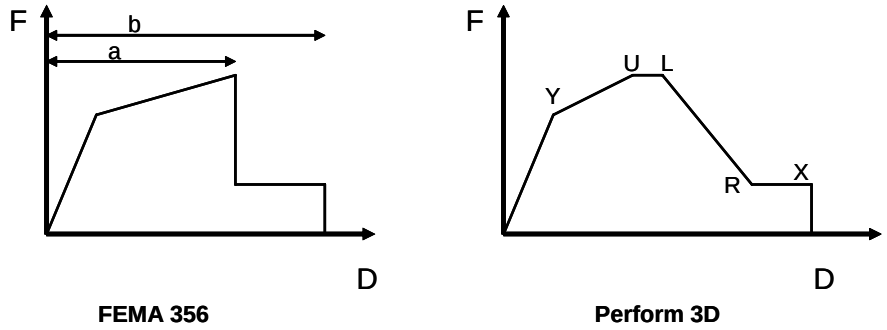

Fig.5 Comparison of load deformation relationships (left = FEMA, right = Perform3D)

Strength Calculations and Deformation Capacities

Over-strength values recommended by FEMA356 were implemented in the computations. For example, the moment strength of beams was computed using a 1.25 increase for the steel yield stress and 1.5 for concrete compressive strength. Calculations were done using a resistance factor of unity. Plastic hinge rotations corresponding to the onset of strength degradation and ultimate failure, as shown by parameters “a” and “b” in fig.5 are tabulated in FEMA 356 as a function of condition of transverse reinforcement, shear force on the member, percentage of tensile and compressive reinforcement and axial force (in columns). A thorough analysis for each different section was done and strength and deformations were obtained and modeled.

Nonlinear Dynamic Analysis (NDA) and Observer Estimates

Fig.6 (left) compares the open loop model prediction of the acceleration at the roof in the E-W direction due to Northridge with the measurement from ch1. As can be seen, the comparison is reasonable indicating that the model captures the basic features of the behavior, at least within the amplitude of the observed response. Needless to say, one does not expect the nonlinear model to give the “true” response so the targets used to judge the predictive capability

of NSP are not, as noted previously, the open loop model predictions but observer estimates. The improvements realized by the observer can be appreciated by inspecting the right side of fig.6 which shows the estimate obtained with the observer when the measurements at the roof are removed from the feedback. As can be seen, the improvement, which is a lower bound because is based on use of less than all the available information, is important.

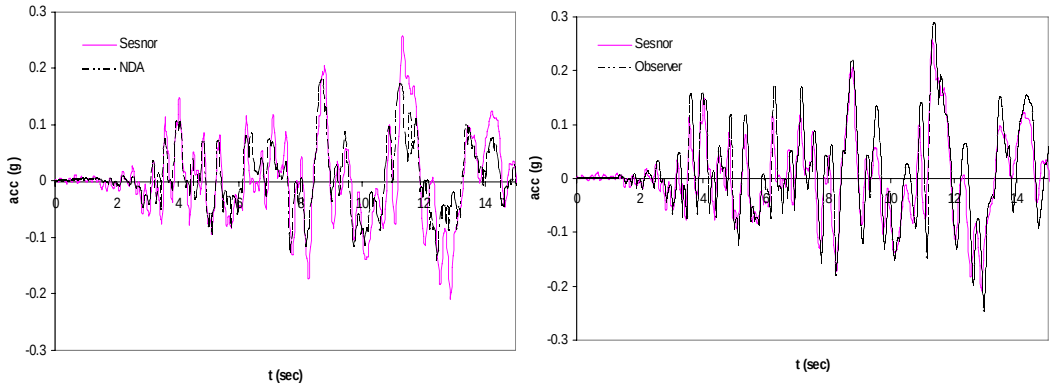

Fig.6 Ch1 acceleration in E-W direction a) NDA vs. measurements b) Observer prediction vs. measurement (obtained discarding the roof measurements)

Performance Points and Quantities of Interest

Three different load patterns are considered: LP1= code based triangular load distribution; LP2= distribution proportional to the fundamental mode and LP3 = uniform distribution. The pushover analysis is carried out on the loaded structure so a static analysis under gravity load precedes the pushover analysis. FEMA 356 requires consideration of two gravity load combinations 1.1(D + L) and 0.9D. The mass of the structure (for inertial purposes) was taken as the mass from the dead load plus 5 percent of the live load. Concurrent seismic effects for each load pattern were considered applying simultaneously 100% of loads in the primary direction under consideration plus 30% of the loads from the other direction. The results for the Northridge earthquake are presented in Tables 3 and 4 and in fig 7. A representative pushover plot is shown in fig.8.

Table 3 Performance Point in longitudinal direction

Method	Load Pattern 1				Load Pattern 2				Load Pattern 3			
	Sa (g)	Sd (in)	V/W	drift %	Sa (g)	Sd (in)	V/W	drift %	Sa (g)	Sd (in)	V/W	drift %
ATC 40	0.103	8.507	0.085	0.52	0.1001	7.483	0.090	0.48	0.1176	6.591	0.097	0.40
FEMA 440 (Linearization)	0.116	9.650	0.089	0.60	0.1069	9.447	0.097	0.59	0.1108	9.690	0.110	0.56
FEMA 356 (CM)	0.109	11.680	0.093	0.72	0.1098	10.670	0.100	0.66	0.1201	9.786	0.111	0.58
FEMA 440 (CM)	0.119	10.790	0.091	0.66	0.1100	10.460	0.099	0.65	0.1145	10.650	0.113	0.62

Table 4 Performance Point in transverse direction

Method	Load Pattern 1				Load Pattern 2				Load Pattern 3			
	Sa (g)	Sd (in)	V/W	d %	Sa (g)	Sd (in)	V/W	d %	Sa (g)	Sd (in)	V/W	d %
ATC 40	0.100	8.330	0.074	0.53	0.0919	7.404	0.074	0.48	0.1027	5.926	0.076	0.37
FEMA 440 (Linearization)	0.104	8.465	0.076	0.54	0.0966	8.025	0.078	0.53	0.0926	7.675	0.089	0.47
FEMA 356 (CM)	0.103	9.707	0.080	0.60	0.1004	9.041	0.082	0.57	0.1082	7.771	0.091	0.47
FEMA 440 (CM)	0.109	8.916	0.078	0.57	0.1006	8.634	0.082	0.56	0.1013	9.018	0.098	0.54

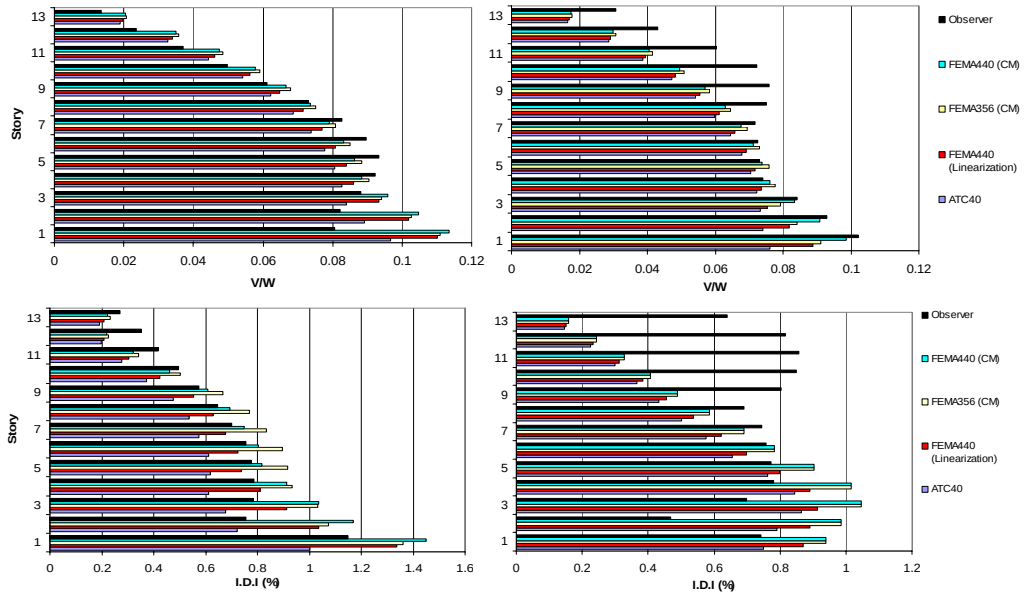

Fig.7 NSP predictions: shears on top inter-story drift index bottom: E-W and N-S (left and right)

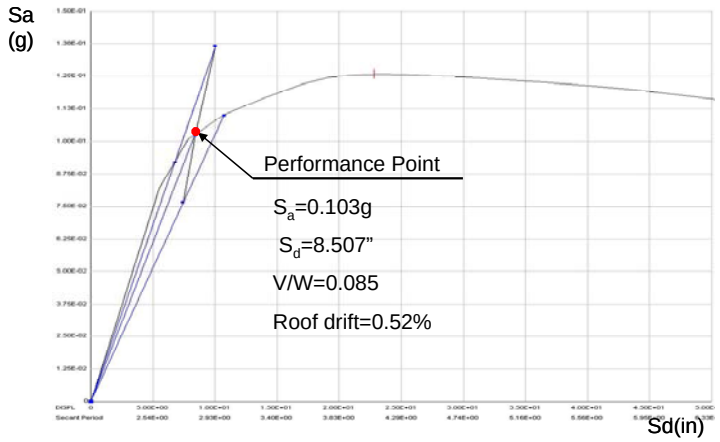

Fig.8 Pushover curve for SO building (LP1 in longitudinal direction, ATC-40 method)

Observations

- The differences between the estimates of the observer and the predictions of the various NSP are of the same order, although there is a small improvement in the modified versions presented in FEMA-440.
- Errors in the inter-story shears are typically less than 20% with two exceptions. A conservative estimate in E-W for the lower two floors and a significantly unconservative estimation in the upper floors in the N-S direction. This last item is easily rationalized by looking at the spectrum of the motion which shows large relative amplitudes at shorter periods and thus much more significant higher mode effects in the N-S direction (fig.9).
- Underestimation of the drift ratios in the upper floors in the N-S direction is even more pronounced than in shear. These results suggests that during the dynamic response there are instances when the shears in the upper levels are significant and the effective inter-story stiffness is much lower than the value (implicit) in the pushover. This means that

the effective inter-story stiffness is notably dependent on the load distribution, which is not surprising since the beam to column stiffness ratio is low. A detailed discussion on this matter can be found in the final report [3].

- Drifts in the lower two floors in the N-S direction are significantly overestimated, although this is not the case for the associated shears. This result indicates once again that the building has a behavior that is far from that of a shear building idealization.
- It is opportune to note that the Sherman Oaks building is outside the strict range of applicability of the current NSP since the period of the fundamental mode in both directions is larger than 2.0 seconds.

We close by noting that the base shear capacity of the building in the short direction is 0.12W (including material over-strength) and that when the response base shear is computed with simple methods (such as linear interpolation of accelerations) base shears much larger than this are computed. This result points to the importance of estimating the "measured" quantities carefully since otherwise misleading observations can result.

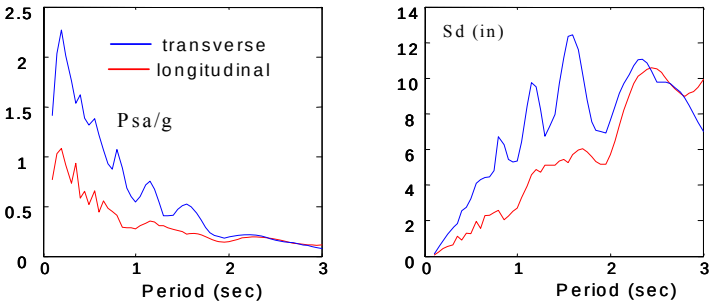

Fig 9. Elastic spectra for 5% damping (left = pseudo acceleration, right = displacement)

Imperial County Services

The 6-story imperial county services building (CSMIP station number -1260) in El-Centro CA was built in 1969. In 1979 it suffered heavy damage from the magnitude 6.5(M_L) Imperial Valley earthquake and was subsequently demolished. A detailed description of the building and information on the extent of the damage can be found in ATC-09 [14]. Fig.10 illustrates floor plans showing the configuration of the shear walls and fig.11 shows the instrumentation set up.

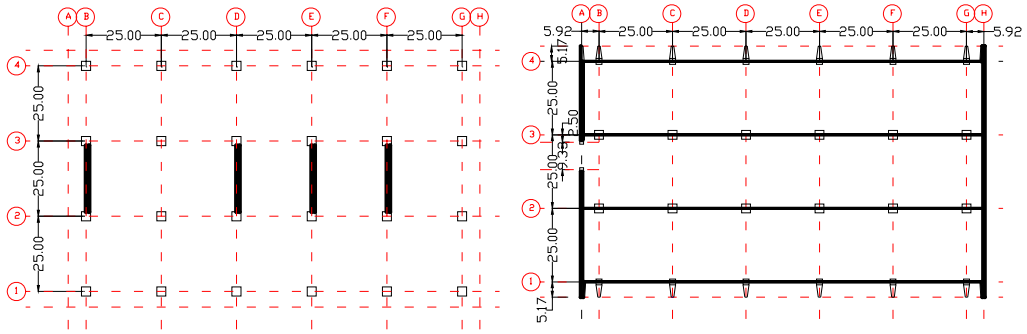

Fig.10 (left) plan view of the ground level, (right) typical plan view of stories two and above

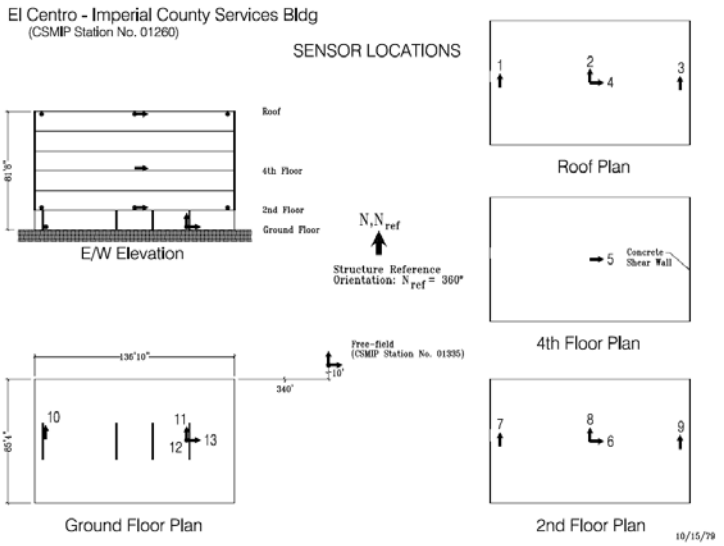

Fig.11 Layout of the sensors installed at ICS building (taken from CSMIP web site).

System Identification and dynamic properties

The only available ground motion record on this building is the one that resulted in the heavy damage. The quasi-linear properties of the building were estimated using the early portion of the record (prior to the initiation of damage). Given the rather short time available, however, it only proved feasible to identify the fundamental mode in each direction. The results obtained are summarized in Table 5.

Table 5 Identified modal properties of the ICS building

Direction	T (sec)	ζ (%)
Longitudinal (X)	0.80	5
Transverse (Y)	0.44	8

Analytical model and updating

Nonlinear behavior was modeled by lump plasticity in the members of the rigid frames located above the first level, while nonlinear fiber elements were used to model the walls and the columns in level #1. The elastic periods were found to be 0.84 sec in the longitudinal and 0.47 sec in the transverse direction, which are quite close to the identified values. Since the variance associated with the identified values is relatively large (due to the short available time) it was decided to use the model as formulated. In this building the item that is of paramount importance is modeling the strength degradation characteristics of the critical regions. The possibility for concrete crushing and steel bar buckling was considered. The biaxial nature of the motion is also critical in this case and was considered in all the analyses. Nominal material strengths were increase by 1.5 (concrete) and 1.25 (steel).

Nonlinear Dynamic Analysis

The 3D model of the building, when subjected to the recorded biaxial ground accelerations predicts an axial-flexural failure of the corner column on line G. This result matches the actual failure mode. Fig.12 shows the first 10 seconds of the acceleration response at the roof in the longitudinal and transverse direction and compares it with the measured values. As can be seen, the model tracks the measurements rather well up to about seven seconds which is the time when the northwest corner column fails. Comparisons beyond the time of failure are not meaningful since the model cannot be expected to track the post-failure state.

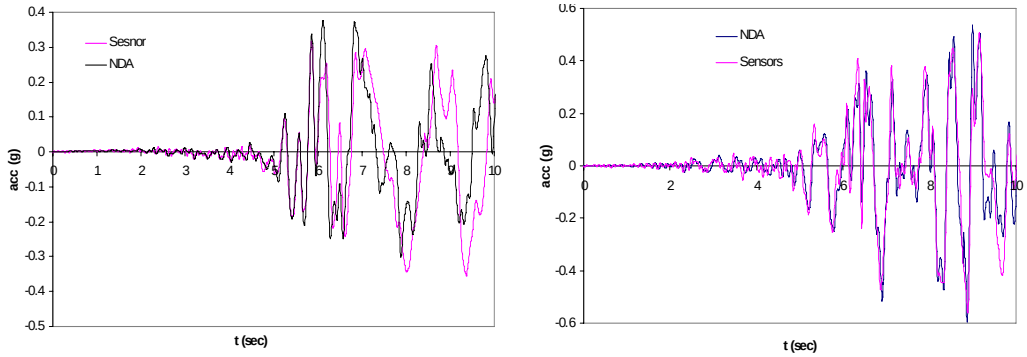

Fig.12 Acceleration response at the roof: (left) ch4, (right) ch2

Nonlinear Static Procedure and Evaluation of the Performance Point

Fig.13 illustrates a typical pushover curve in the longitudinal direction and the performance point for the case of the ATC-40 equivalent linearization method. As can be seen, the point falls on the softening part of the curve showing that failure is predicted. Results for all the other techniques and load distributions are summarized in Tables 6 and 7.

Table 6 Performance point evaluation in Longitudinal direction

Method	Load Pattern 1				Load Pattern 2				Load Pattern 3			
	Sa (g)	Sd (in)	V/W	drift %	Sa (g)	Sd (in)	V/W	drift %	Sa (g)	Sd (in)	V/W	drift %
ATC 40	0.208	6.264	0.165	0.79	-	-	-	-	0.278	3.339	0.219	0.42
FEMA 440 (Linearization)	0.247	3.166	0.195	0.41	0.233	3.301	0.197	0.43	0.257	3.188	0.250	0.41
FEMA 356 (CM)	0.243	3.445	0.188	0.44	0.232	3.488	0.192	4.62	0.303	2.822	0.254	0.36
FEMA 440 (CM)	0.244	3.290	0.192	0.42	0.231	3.369	0.196	0.44	0.257	3.273	0.228	0.41

Table 7 Performance point evaluation in Longitudinal direction

Method	Load Pattern 1				Load Pattern 2				Load Pattern 3			
	Sa (g)	Sd (in)	V/W	d %	Sa (g)	Sd (in)	V/W	d %	Sa (g)	Sd (in)	V/W	d %
ATC 40	0.449	1.896	0.373	0.23	0.458	1.724	0.409	0.22	0.366	2.349	0.302	0.29
FEMA 440 (Linearization)	0.410	2.844	0.352	0.26	0.477	1.817	0.415	0.24	0.323	2.840	0.379	0.26
FEMA 356 (CM)	0.412	2.793	0.334	0.28	0.520	2.094	0.430	0.26	0.389	2.716	0.456	0.20
FEMA 440 (CM)	0.425	2.997	0.345	0.26	0.508	2.133	0.444	0.28	0.328	2.964	0.362	0.27

Observations

- All four NSP were able to predict the observed failure.
- Convergence of ATC-40 for LP2 in the longitudinal direction proved impossible, which once again points to failure.

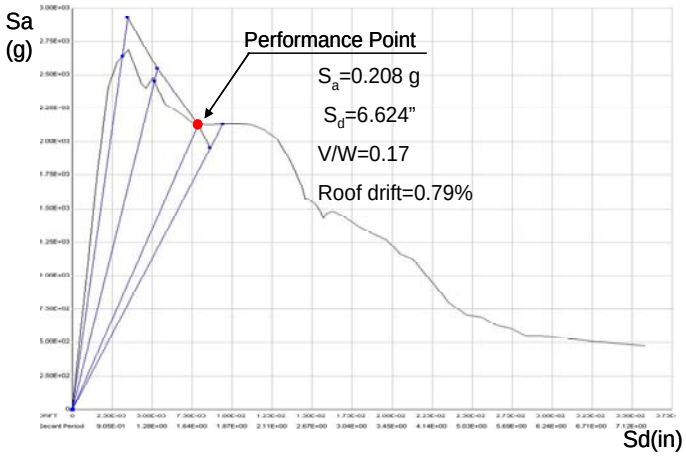

Fig.13 Performance point in longitudinal direction under LP1 by ATC-40 method

Telephone Building in Watsonville

This building (CSMIP station 47459) was designed in 1948 and was initially build with three stories. The fourth level was added in 1955. The vertical load resisting system is concrete slabs supported by composite steel-concrete frames and the main lateral load resisting system consists of a number of solid and perforated shear walls. The foundation system is made of spread and strip footings over alluvium. Figure 14 shows the instrumentation layout.

Soil Structure Interaction

Elastic spectra for the two available records are depicted in the E-W direction in fig.15. The Loma Prieta earthquake (LP) produced much larger response than Morgan Hill (MH) and for this reason we limit our discussions to Loma Prieta. Looking at the LP spectrum one can see two peaks bellow 0.4 seconds that are associated with feedback from strong SSI effects.

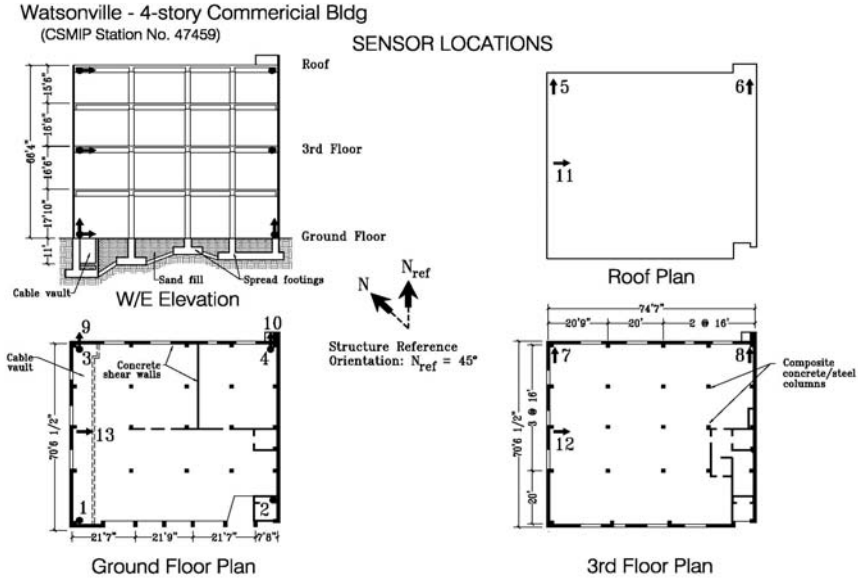

Fig.14 Instrumentation layout of Watsonville building (taken from CSMIP website)

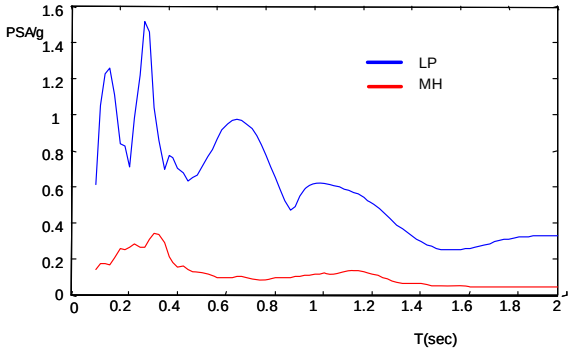

Fig15. Elastic spectra for 5% damping in the E-W direction

There are 4 vertical accelerometers at the base. To test the typical assumption of base rigidity the acceleration in ch4 was computed from the results at sensors 1, 2 and 3 (using the rigid premise) and the Fourier Spectrum of the result is compared to that of the measurements in fig.16. The result shows that the rigid assumption is accurate for frequencies up to about 2 Hz but for higher frequencies it is less accurate, especially near the resonant frequencies of the structure. While the use of the term rocking carries the rigid plane assumption one can compute approximate rocking components by least square fitting a plane to the vertical accelerations and taking the rocking as the rotations of this plane. Fig.17 shows that the contribution of this "pseudo-rocking" to the total roof acceleration is substantial.

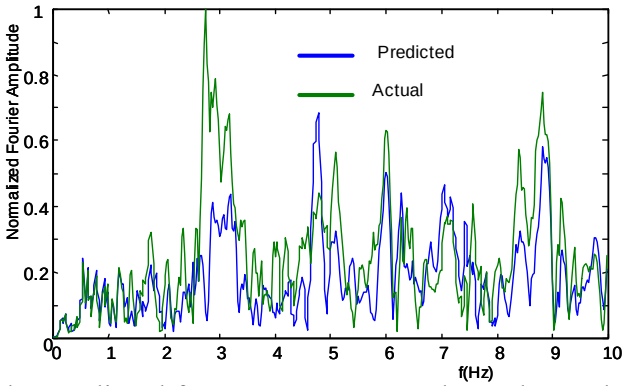

Fig.16 Spectrum of ch4 predicted from sensors 1, 2 and 3 and actual measurement (LP record).

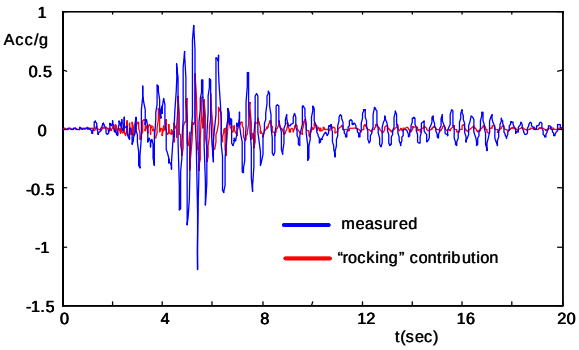

Fig.17 Acceleration in ch11 (E-W roof) for LP excitation

System Identification

The Morgan-Hill motion was used to perform the ID because this record is the less intense of the two available and thus "quasi-linear" behavior is more closely realized. Subspace identification and the Observer Kalman Filter ID were tried but both gave results that showed significant dependency on the initial order selected, in all likelihood because the feedback effects make the input and output spectra have coincident peaks. Use of reversed time Markov Identification, however, lead to robust results. The basic idea in reversed time analysis is to flip the problem mathematically so that the stable modes become unstable. The results from the reversed time identification are: $f_{E\text{-}W} = 3.62$ Hz $\phi = [1, 0.52]^T$, $f_{N\text{-}S} = 4.95$ Hz, $\phi = [1, 0.61]^T$. It is worth noting that the mode shapes in both directions are close to straight lines (at least based on the available points), which supports the previous observation regarding the fact that a significant part of the deformation is coming from base rotation.

Analytical model and updating

To model SSI, spring and dashpots were introduced at the base. Relative values of the parameters were determined using the geometry of the foundation and the scaling was selected based on the identified frequencies. It was found that the scaling selected corresponded to a modulus of subgrade reaction of 120k/ft^3. The natural frequencies of the model in the E-W and N-S directions are 3.66 Hz and 4.88 Hz. Nonlinearity, and strength loss in shear in the walls, was considered in the model. Fig.18 shows a comparison of roof acceleration obtained from NDA analysis with measured data which illustrates that the model is reasonably accurate.

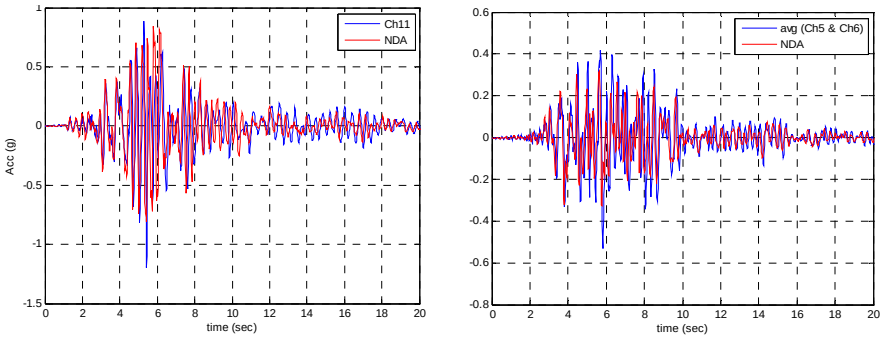

Fig.18 NDA acceleration vs measurements (left) E-W (right) N-S (LP records)

Evaluation of the Performance Points

ATC40 and FEMA 356 adopt a simplified approach to account for SSI that considers base flexibility but not the increase in damping that arises from radiation. FEMA 440, however, offers a method to account for both effects. Table 8 summarizes the total damping due to SSI that is used in the NSP. For nonlinear dynamic analysis we included radiation damping by adding βK damping to the foundation springs; details are presented in [3].

Table 8 Effective damping due to SSI, used in FEMA 440 methods

Direction	Structural Damping β 1 %	FoundationDamping β f %	total SSI damping β 0 %
Longitudinal (X)	5	1.99	5.36
Transverse (Y)	5	4	7

Tables 9 and 10 show the performance point evaluations in E-W and N-S directions for the Loma Prieta event. A representative push over curve with a performance point computation is depicted in fig.19 and the key results are summarized in fig.20.

Table 9 Performance point evaluation in Longitudinal (X) direction

Method	Load Pattern 1				Load Pattern 2				Load Pattern 3			
	Sa (g)	Sd (in)	V/W	drift %	Sa (g)	Sd (in)	V/W	drift %	Sa (g)	Sd (in)	V/W	drift %
ATC 40	0.661	0.682	0.339	0.109	0.6151	0.734	0.339	0.122	0.677	0.599	0.348	0.096
FEMA 440 (Linearization)	0.645	0.817	0.360	0.121	0.6257	0.835	0.349	0.136	0.633	0.811	0.372	0.107
FEMA 356 (CM)	0.627	0.686	0.340	0.109	0.6020	0.725	0.343	0.125	0.647	0.628	0.349	0.096
FEMA 440 (CM)	0.646	0.831	0.363	0.128	0.6267	0.853	0.352	0.144	0.636	0.818	0.385	0.118

Table 10 Performance point evaluation in Transverse (Y) direction

Method	Load Pattern 1				Load Pattern 2				Load Pattern 3			
	Sa (g)	Sd (in)	V/W	drift %	Sa (g)	Sd (in)	V/W	drift %	Sa (g)	Sd (in)	V/W	drift %
ATC 40	0.577	0.259	0.304	0.050	0.535	0.314	0.293	0.054	0.589	0.231	0.290	0.037
FEMA 440 (Linearization)	0.575	0.391	0.316	0.056	0.552	0.359	0.304	0.058	0.580	0.001	0.354	0.055
FEMA 356 (CM)	0.597	0.365	0.307	0.051	0.569	0.350	0.297	0.056	0.630	0.336	0.334	0.047
FEMA 440 (CM)	0.585	0.411	0.323	0.058	0.579	0.402	0.321	0.066	0.608	0.429	0.365	0.059

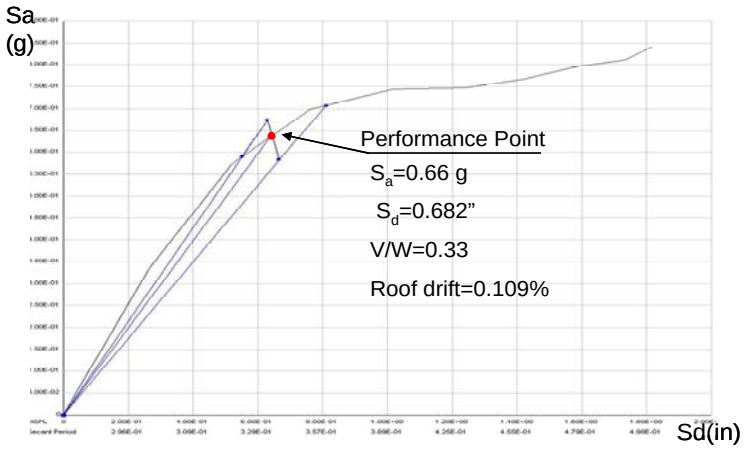

Fig.19 Performance point in longitudinal direction under LP-1 by ATC-40 method

Predictive Capability of NSP

The mean and the coefficient of variation of the ratio of predictions to measurements are depicted in fig.21 for all the data available. The mean in the shears are not far from unity and the coefficient of variation, although not small at around 0.22, is "tolerable". More or less the same assertion can be made for the overall displacements but the drift indices, however, are under-predicted in the mean and a representative *cv* is around 0.45, indicating a rather large spread. Although not shown here, the computation of the same statistics with the data segregated into the upper half and the lower half of the buildings shows that the accuracy in the lower half is notably better than the average and, of course, significantly worst on the upper floors. This result can be

rationalized by noting that the higher mode contributions tend to be larger in the upper levels. Differences between the various techniques do not appear statistically significant.

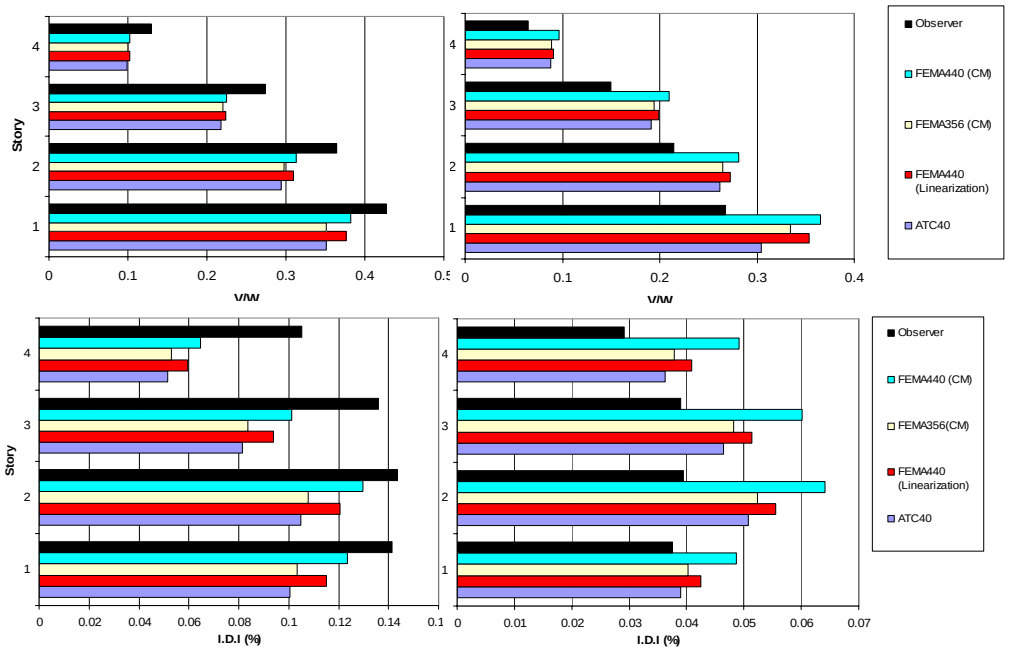

Fig.20 NSP predictions and observer predictions: (top) shears (bottom) inter-story drift index- E-W on left N-S on right.

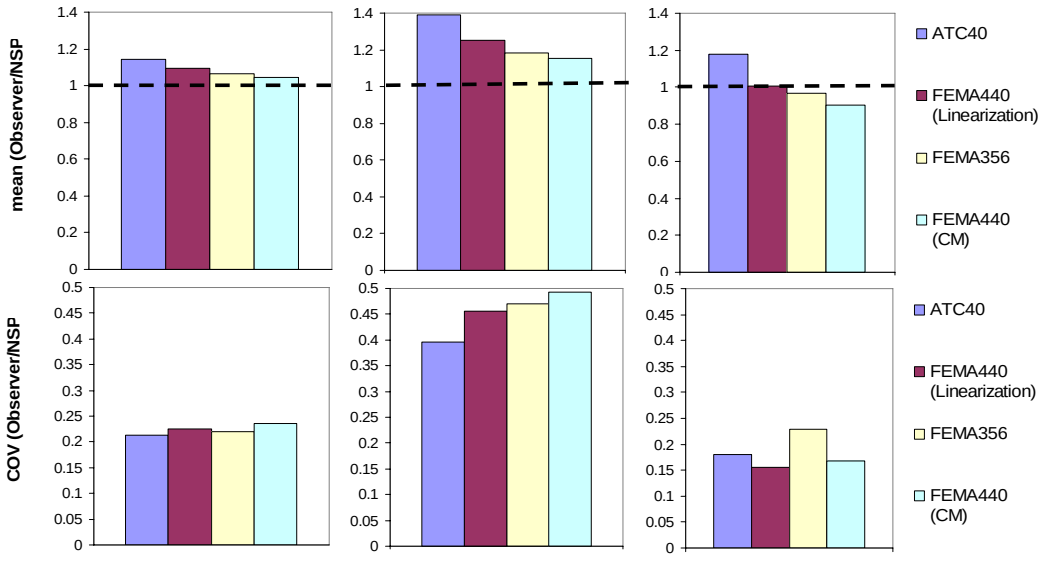

Fig.21 Ratio of observer to NSP predictions – mean on the top and *cv* on bottom – shears on left column, drift indices on center and total displacements on right.

Concluding Comments

The results obtained in this project support the contention that the accuracy of current NSP is significantly higher in the lower floors than in the upper floors of buildings. For example, the coefficients of variation for shears and drift indices were found to be {0.45 and 0.22} when computed over all levels and {0.2 and 0.14} when only the data on the lower half of the buildings is considered. Since the lower levels are often critical this is a good sign yet it appears that there is room for improvement in upper floor performance. Although NSP are necessarily approximate (since the true complexity of the nonlinear dynamic response does not fit within the framework) the results obtained in this project suggest that they can be "sufficiently accurate" to identify important deficiencies and thus point to appropriate retrofit strategies. In closing it is opportune to emphasize that a necessary condition for any NSP to succeed is that the model used to represent the building be accurate (enough) and, in particular, that it be able to capture all the important sources of strength and stiffness degradation. An excellent example pointing to this fact is the Imperial County Services Building, where all NSP predict failure when the poorly confined concrete in the columns of the first story is properly modeled but neither can reproduce the observed behavior if this is not the case. Several other examples of this same point, not included in this paper due to space constraints, can be found in the final report [3].

Acknowledgement

The research reported in this paper was supported by the California Strong Motion Instrumentation Program (CSMIP) through Standard Agreement N0. 1005-834, this support is gratefully acknowledged.

References

[1] ATC-55 (2005). *Applied Technology Council*, Redwood City, CA

[2] Hernandez E., and Bernal D. "State estimation in systems with uncertain damping and stiffness properties", *Journal of Engineering Mechanics*, ASCE (in press).

[3] Bernal D. (2007). Predictive capability of nonlinear static analysis procedures for seismic evaluation of buildings, CSMIP *report on data interpretation project*.

[4] Husid, R. (1967). Gravity effects on the earthquake response of yielding structures, *Earthquake Engineering Research Laboratory*, California Institute of Technology, Pasadena.

[5] Jennings P.C. and Husid, R. (1968). "Collapse of yielding structures under earthquakes", *Journal of Engineering Mechanics*, ASCE, Vol. 94, No.5, pp.1045-1065.

[6] Bernal, D. (1992)."Instability of buildings subjected to earthquakes", *Journal of Structural Engineering*, ASCE, Vol. 18, No.8, pp. 2239-2260.

[7] Bernal, D. (1998). "Instability of buildings during seismic response", *Engineering Structures,* Vol.20, No.4-6, pp.496-502.

[8] FEMA 440 (2005), *Improvement of nonlinear static seismic analysis procedures*, prepared by Applied Technology Council for the Federal Emergency Management Agency, Washington, D.C.

[9] FEMA 356 (2000), *Prestandard and Commentary for the Seismic Rehabilitation of Buildings*, prepared by the American Society of Civil Engineers for the Federal Emergency Management Agency, Washington, D.C.

[10] Juang, J. (1994), *Applied system identification*, Prentice-Hall, Upper Saddle River, N.J.

[11] Naeim,F. (1998), "Performance of 20 extensively-instrumented buildings during the 1994 Northridge earthquake", *Structural Design of Tall Buildings*, Vol. 7, No. 3, pp. 179-194

[12] Van Overschee, P., and Moor,B.L. (1996). Subspace identification for linear systems: Theory, implementation and applications, Kluwer Academics, Boston MA.

[13] Pappa R.S. and Elliott K.B., (1993). "Consistent-mode indicator for the eigensysytem realization algorithm", *Journal of Guidance, Control and Dynamics*, Vol.16 No. 5, pp. 852-858.

[14] ATC-9 (1984). An Evaluation of the Imperial County Services Building Earthquake response and Associated Damage, *Applied Technology Council*, Redwood City, CA.